

2,6-Diiminopyridine Complexes of Group 2 Metals: Synthesis, Characterisation and Redox Behaviour

Michael J. C. Dawkins¹, Alexandr N. Simonov^{1,2*} and Cameron Jones^{1*}

¹School of Chemistry, PO Box 23, Monash University, VIC, 3800, Australia.

² ARC Centre for Electromaterials Science, Monash University, VIC, 3800, Australia

Supplementary Information (18 pages)

Contents	1. Experimental	S2
	2. X-Ray Crystallography	S9
	3. Electrochemical Studies	S14
	4. References	S18

1. Experimental

General considerations.

All manipulations were carried out using standard Schlenk and glove box techniques under an atmosphere of high purity dinitrogen. Diethyl ether was distilled over Na/K alloy (50:50), while hexane, toluene and THF were distilled over molten potassium. ^1H NMR spectra were recorded on either Bruker AvanceIII 600, Bruker AvanceIII 400 or Bruker AvanceI 300 spectrometers. ^1H NMR spectra were referenced to the resonances of the solvent used. Mass spectra were collected using an Agilent Technologies 5975D inert MSD with a solid-state probe. FTIR spectra were recorded as Nujol mulls, using an Agilent Cary 630 spectrometer operating in attenuated total reflectance (ATR) or transmission modes. The UV/visible spectrum was recorded on a Cary 1E spectrometer. It is of note, however, that the extreme air sensitivity of the highly coloured reduced $^{\text{Ph}}\text{Dimpy}$ complexes generally precluded the acquisition of such spectra. Microanalyses were carried out at the Science Centre, London Metropolitan University. Melting points were determined in sealed glass capillaries under dinitrogen, and are uncorrected. The starting materials $^{\text{Ph}}\text{Dimpy}$,¹ $[\{(\text{Mes})\text{Nacnac}\}\text{Mg}\}_2]$ ² and KC_8 ³ were prepared by literature procedures. $[\text{MgI}_2(\text{OEt}_2)_2]$ was prepared by treating magnesium powder with 1 equivalent of I_2 in diethyl ether. All other reagents were used as received.

Synthesis of $[(^{\text{Ph}}\text{Dimpy})\text{MgI}_2]$ **4.** Considering the very low solubility of **4**, the following synthetic method was utilised to obtain the compound as an analytically pure crystalline solid. Two solutions, $[\text{MgI}_2(\text{OEt}_2)_2]$ (141 mg, 0.33 mmol) in 5 mL of diethyl ether, and $^{\text{Ph}}\text{Dimpy}$ (200 mg, 0.33 mmol) in 5 mL of toluene, were placed on either side of a custom built Schlenk H-tube flask. The remaining volume on each side of the flask was layered with the corresponding solvent (*ca.* 3 mL each), until the two solvents met in the diffusion cross-tube. The tube was left for three weeks, allowing the two solutions to diffuse together. Yellow crystals of **4** formed in the middle of the cross-tube. The reaction solution was decanted from the crystals, which were subsequently dried under vacuum. (175 mg, 60%). MP: >260 °C; ^1H NMR (600 MHz, C_6D_6 , 298 K) δ = 0.93 (d, J = 6.0 Hz, 12H, $\text{CH}(\text{CH}_3)_2$), 1.68 (d, J = 6.0 Hz, 12H, $\text{CH}(\text{CH}_3)_2$), 3.50 (br. m, 4H, $\text{CH}(\text{CH}_3)_2$), 6.79-7.17 (m, 19H, Ar-H); N.B. The very low solubility of the compound in non-coordinating solvents precluded the acquisition of meaningful ^{13}C NMR spectroscopic data; MS/EI m/z (%): 605.5 ($^{\text{Ph}}\text{Dimpy}^+$, 88), 528.5 ($^{\text{Ph}}\text{Dimpy-Ph}^+$, 12), 264.1 (PhC=NDip^+ , 100), 176.2 (N(H)Dip^+ , 83); anal. calc for $\text{C}_{43}\text{H}_{47}\text{N}_3\text{MgI}_2$: C 58.43%, H 5.36%, N 4.75%, found: C 58.33%, H 5.25%, N 4.91%.

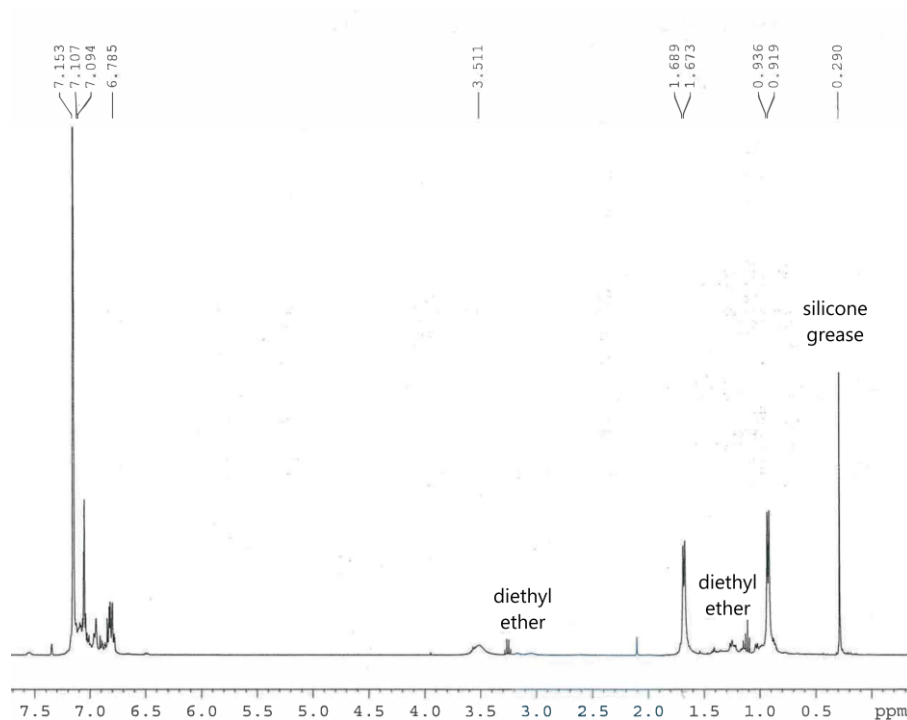


Figure S1. ^1H NMR spectrum (600 MHz, 298 K, C_6D_6) of **4**.

Synthesis of [$^{\text{Ph}}\text{Dimpy}\cdot\text{MgI}$] **5. **Route 1:** To a solution of $[\text{MgI}_2(\text{OEt}_2)_2]$ (211 mg, 0.495 mmol) in 10 mL diethyl ether was added $^{\text{Ph}}\text{Dimpy}$ (300 mg, 0.495 mmol) in 10 mL toluene with rapid stirring, instantly forming a yellow precipitate. The suspension was stirred for 3 h, and subsequently added dropwise over 5 minutes to a slurry of KC_8 (67 mg, 0.495 mmol) in 5 mL of toluene at -80 $^\circ\text{C}$. The reaction mixture was warmed slowly to room temperature and stirred for 18 h. The resultant dark red solution was filtered from the insoluble graphite and potassium iodide. Concentration (*ca.* 10 mL) and storage at -30 $^\circ\text{C}$ for 18 h yielded **5** as red crystals. The mother liquor was decanted and the crystalline product dried under vacuum (252 mg, 67%). **Route 2:** To a solution of $[\text{MgI}_2(\text{OEt}_2)_2]$ (211 mg, 0.495 mmol) in 10 mL diethyl ether was added $^{\text{Ph}}\text{Dimpy}$ (300 mg, 0.495 mmol) in 10 mL toluene with rapid stirring, instantly forming a yellow precipitate. The suspension was stirred for 3 h, and then cooled to -80 $^\circ\text{C}$. To the cooled suspension was added a solution of $[\{(\text{Mes})\text{Nacnac}\}\text{Mg}]_2$ (177 mg, 0.247 mmol) in 10 mL toluene over 5 minutes. The reaction mixture was warmed slowly to room temperature and stirred for 4 h, then placed in the freezer for 18 h to allow the generated $[(\text{Mes})\text{Nacnac}\}\text{MgI}(\text{OEt}_2)]$ to precipitate. The resultant dark red solution was then filtered. Concentration (*ca.* 10 mL) and storage at -30 $^\circ\text{C}$ for 18 hr yielded **5** as red crystals. The mother liquor was decanted and the crystalline product dried under vacuum (232 mg, 62%). MP: >260 $^\circ\text{C}$ (dec.); ^1H NMR (300 MHz, C_6D_6 , 298 K) δ = 1.42 (br.), 2.02 (v. br.), 3.57 (v. br.), 6.75 (br.), 7.03 (br.); N.B. no signals were observable in the ^{13}C NMR spectrum of the paramagnetic compound; MS/EI *m/z* (%): 605.6 ($^{\text{Ph}}\text{Dimpy}^+$, 15), 264.3 (PhCNDip^+ , 15), 160.2**

(Dip-H⁺, 100); anal. calc for C₄₃H₄₇N₃MgI: C 68.22%, H 6.26%, N 5.55%, found C 67.97%, H 6.11%, N 5.46%.

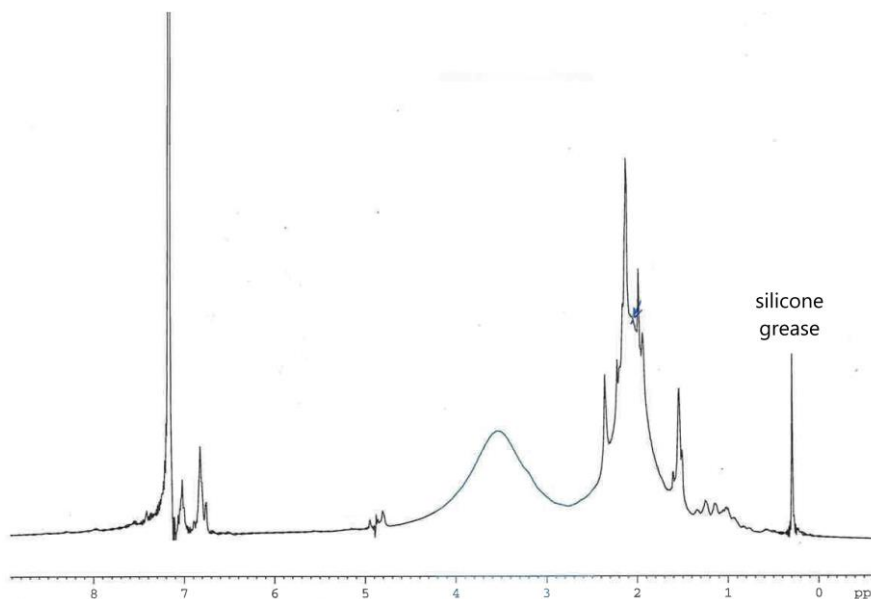


Figure S2. ¹H NMR spectrum (300 MHz, 298 K, C₆D₆) of **5**.

Synthesis of [(^{Ph}Dimpy)Mg(OEt)₂] **6. Route 1:** To a solution of [MgI₂(OEt)₂] (2.44 g, 5.72 mmol) in 30 mL diethyl ether was added ^{Ph}Dimpy (3.15 g, 5.20 mmol) in 50 mL toluene with rapid stirring, instantly forming a yellow precipitate. The suspension was stirred for 3 h, and subsequently added over 5 minutes to a slurry of KC₈ (1.54 g, 11.44 mmol) in 20 mL toluene at –80 °C. The reaction mixture was warmed slowly to room temperature and stirred for 18 h. The resultant purple solution was filtered from the insoluble graphite and potassium iodide. Concentration (*ca.* 10 mL) and storage at –30 °C for 18 h yielded **6** as dark red crystals. The mother liquor was decanted and the crystalline product dried under vacuum (2.35 g, 64%). **Route 2:** Magnesium metal powder (2.01 g, 8.25 mmol) was suspended in 30 mL diethyl ether, and activated by the addition of a single crystal of iodine (*ca.* 5 mg). Once the solution returned to colourless, a solution of ^{Ph}Dimpy (10.00 g, 1.65 mmol) in 70 mL toluene was added rapidly at room temperature. The reaction mixture was stirred for 18 h, yielding a dark blue solution. The solution was filtered, and volatiles removed under vacuum. The dark purple residue was washed with hexane (*ca.* 20 mL), yielding **6** as a dark purple powder (11.07 g, 99%) MP: >260 °C (dec.); ¹H NMR (300 MHz, C₆D₆, 298 K) δ = 0.32 (br. s, 6H, OCH₂CH₃), 0.92 (d, *J* = 6.3 Hz, 12H, CH(CH₃)₂), 1.08 (d, *J* = 6.0 Hz, 12H, CH(CH₃)₂), 2.85 (br. s, 4H, OCH₂CH₃), 3.29 (br. s, 4H, CH(CH₃)₂), 5.49 (br. s, 1H py-H), 6.92-7.20 (br. m, 18H, ArH and py-H_m); N.B. no distinguishable resonances were observed in the ¹³C NMR spectrum of the compound; IR (ν/cm⁻¹, ATR): 1584 (m), 1523 (m), 1339 (m), 1260 (w), 1216 (w), 1197 (m), 1049 (w), 1017 (m), 929 (w), 855 (w), 758 (m); UV-vis (toluene) [λ_{max}, nm (ε, mol⁻¹ L cm⁻¹): 585

(2386), 550 (1924); MS/EI m/z (%): 629.6 ($(\text{PhDimpy})\text{Mg}^+$, 5), 605.6 (PhDimpy^+ , 64), 264.3 (PhCNDip^+ , 100), 176.2 (DipNH^+ , 46); anal. calc for $\text{C}_{47}\text{H}_{57}\text{N}_3\text{OMg}$: C 80.15%, H 8.16 %, N 5.97%, found C 80.03%, H 8.05%, N 6.13%.

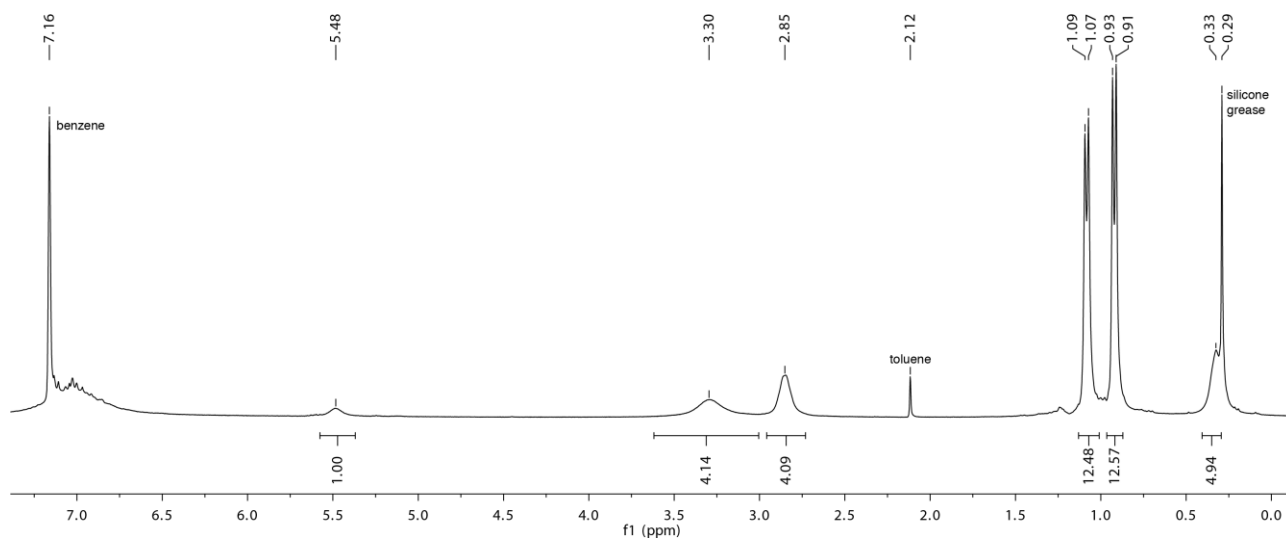


Figure S3. ^1H NMR spectrum (300 MHz, 298 K, C_6D_6) of **6**.

Synthesis of $[(\text{PhDimpy})\text{Mg}(\text{THF})_2]$ **7.** Magnesium metal powder (100 mg, 4.12 mmol) was suspended in 5 mL THF, and activated by the addition of a single crystal of iodine (*ca.* 5 mg), with stirring until the colour of the iodine had disappeared. A solution of PhDimpy (500 mg, 0.825 mmol) in 10 mL of toluene was then added to the magnesium suspension. The reaction mixture was stirred for 18 h at room temperature, and the resultant blue solution was filtered from the excess magnesium metal. The filtrate was concentrated (*ca.* 3 mL), with blue crystals of **7** forming after 18 h. The mother liquor was decanted, and the crystalline product dried under vacuum (568 mg, 89%). MP: >260 °C (dec.); ^1H NMR (400 MHz, C_6D_6 , 298 K) δ = 1.06, 1.17 (br. overlapping, 32H, OCH_2CH_2 and $\text{CH}(\text{CH}_3)_2$), 3.18, 3.44 (br. overlapping, 12H OCH_2 and $\text{CH}(\text{CH}_3)_2$), 5.25 (br. m, 1H py-H), other aromatic proton resonances were difficult to distinguish from the baseline; N.B. no distinguishable resonances were observed in the ^{13}C NMR spectrum of the compound; MS/EI m/z (%): 605.6 (PhDimpy^+ , 59), 264.3 (PhCNDip^+ , 100), 176.2 (DipNH^+ , 87); anal. calc for $\text{C}_{51}\text{H}_{63}\text{N}_3\text{O}_2\text{Mg}$: C 79.10%, H 8.20 %, N 5.43%, found C 78.89%, H 8.02%, N 5.48%.

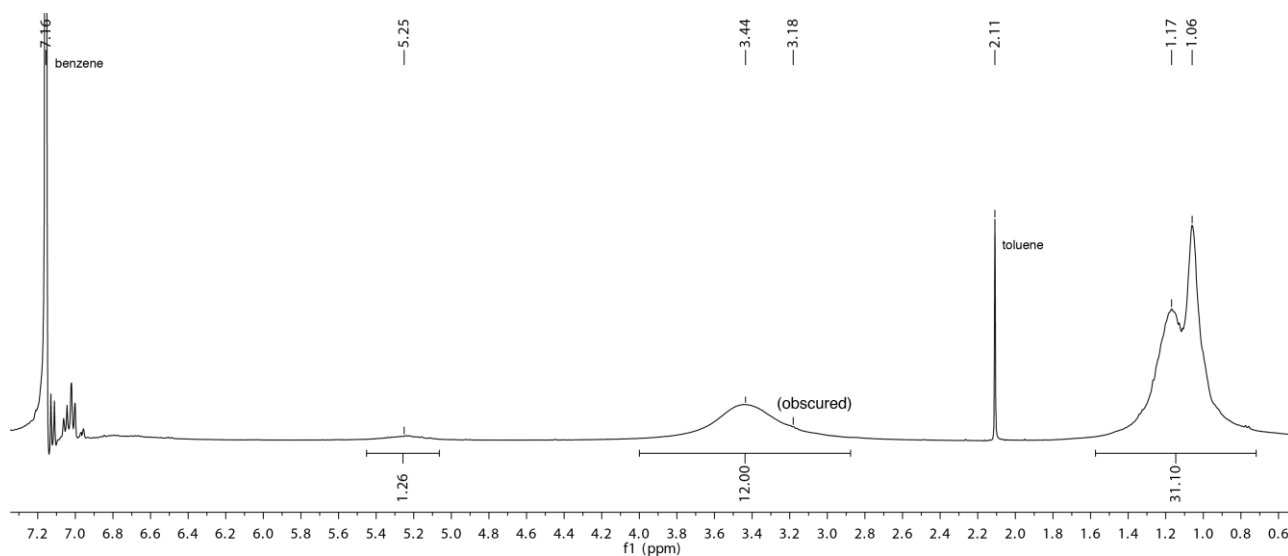


Figure S4. ^1H NMR spectrum (400 MHz, 298 K, C_6D_6) of **7**.

Synthesis of $[(\text{PhDimpy})\text{Ca}]_2$ **8. Route 1:** To a suspension of CaI_2 (0.51 g, 1.73 mmol) in 10 mL diethyl ether was added PhDimpy (1.00 g, 1.65 mmol) in 10 mL toluene with rapid stirring, slowly forming an orange precipitate. The suspension was stirred for 3 h and subsequently added to a slurry of KC_8 (0.49 g, 3.60 mmol) in 20 mL toluene at -80°C . The reaction mixture was slowly warmed to room temperature and stirred for 18 h. The resultant dark brown solution was filtered from the insoluble graphite and potassium iodide. Concentration (*ca.* 3 mL) and storage at room temperature for 18 h yielded **8** as dark red-orange crystals. The mother liquor was decanted and the crystalline product dried under vacuum (630 mg, 59%). **Route 2:** Fresh calcium metal filings (0.13 g, 3.30 mmol) were suspended in 10 mL diethyl ether, and activated by the addition of a single crystal of iodine (*ca.* 10 mg), with stirring until the colour of the iodine had disappeared. A solution of PhDimpy (1.00 g, 1.65 mmol) in 10 mL of toluene was then added to the mixture. The reaction mixture was stirred for 18 h at room temperature, and the resultant black-blue solution filtered from the excess metal. Volatiles were removed under vacuum, and the residue washed with 5 mL of hexane and dried under vacuum, yielding analytically pure **8** as a brown powder (770 mg, 72%). MP: $240\text{--}246^\circ\text{C}$ (dec.); ^1H NMR (300 MHz, C_6D_6 , 298 K) δ = 0.66 (d, J = 6.6 Hz, 6H, $\text{CH}(\text{CH}_3)_2$), 0.68 (d, J = 6.6 Hz, 6H, $\text{CH}(\text{CH}_3)_2$), 0.75 (d, J = 6.6 Hz, 6H, $\text{CH}(\text{CH}_3)_2$), 1.14 (d, J = 6.7 Hz, 6H, $\text{CH}(\text{CH}_3)_2$), 1.19 (d, J = 6.6 Hz, 6H, $\text{CH}(\text{CH}_3)_2$), 1.28 (d, J = 6.7 Hz, 6H, $\text{CH}(\text{CH}_3)_2$), 1.54 (d, J = 6.2 Hz, 6H, $\text{CH}(\text{CH}_3)_2$), 1.79 (d, J = 6.2 Hz, 6H, $\text{CH}(\text{CH}_3)_2$), 2.24 (sept., J = 6.7 Hz, 2H, $\text{CH}(\text{CH}_3)_2$), 2.61 (sept., J = 6.7 Hz, 2H, $\text{CH}(\text{CH}_3)_2$), 4.50 (sept., J = 6.6 Hz, 2H, $\text{CH}(\text{CH}_3)_2$), 4.83 (sept., J = 6.6 Hz, 2H, $\text{CH}(\text{CH}_3)_2$), 5.51 (d, J = 6.6 Hz, 2H, *para*-py-*H*), 6.12 (t, J = 7.2 Hz, 2H, py-*H*), 6.20 (dd, J = 9.1, 6.7 Hz, 2H, py-*H*), 6.54 (t, J = 7.6 Hz, 4H, Ar-*H*), 6.74-7.11 (m, Ar-*H*), 7.30 (t, J = 6.9 Hz, 4H, Ar-*H*), 7.47 (t, J = 9.0 Hz, 6H, Ar-*H*); N.B. The very low solubility of the compound in non-coordinating solvents precluded the acquisition of meaningful ^{13}C NMR

spectroscopic data; MS/EI m/z (%): 605.6 ($^{\text{Ph}}\text{Dimpy}^+$, 47), 264.1 (PhCNDip^+ , 100), 176.2 (DipNH^+ , 97); anal. calc for $\text{C}_{86}\text{H}_{94}\text{N}_6\text{Ca}_2$: C 79.96%, H 7.33%, N 6.51%, found C 79.84%, H 7.47%, N 6.46%.

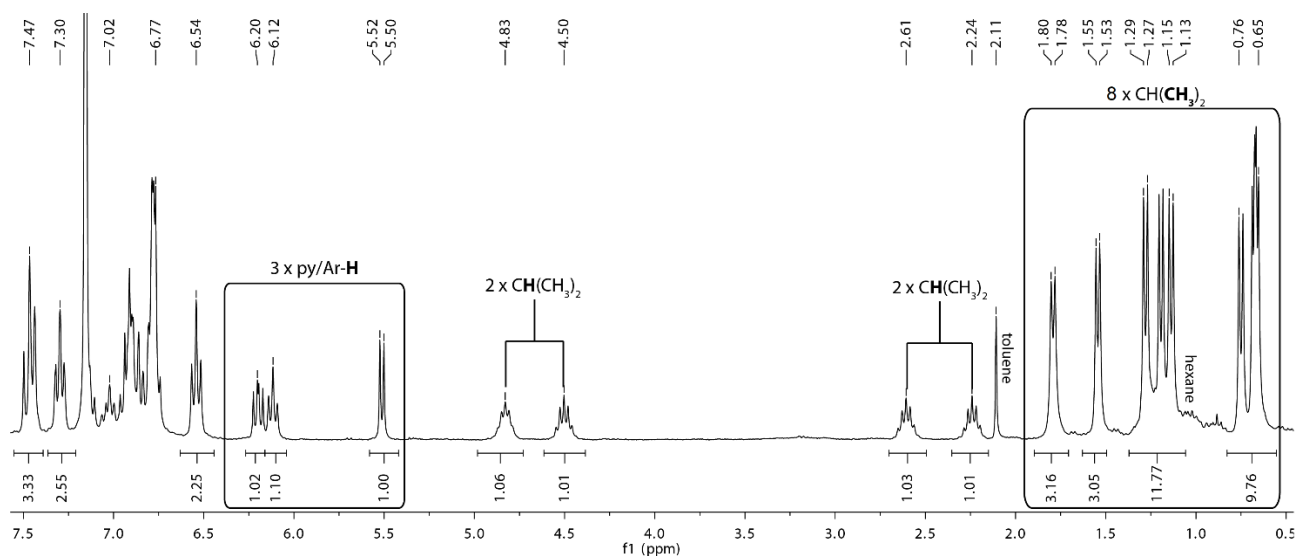


Figure S5. ^1H NMR (300 MHz, C_6D_6 , 298 K) spectrum of **8**, highlighting the number of pyridine and isopropyl proton resonances.

Synthesis of $[\{(\text{PhDimpy})\text{Sr}\}_2]$ **9. **Route 1:** To a suspension of finely ground SrI_2 (186 mg, 0.545 mmol) in 10 mL diethyl ether was added $^{\text{Ph}}\text{Dimpy}$ (300 mg, 0.495 mmol) in 10 mL toluene with rapid stirring. The suspension was stirred for 1 h, and subsequently added to a slurry of KC_8 (147 mg, 1.09 mmol) in 20 mL toluene at -80 °C. The reaction mixture was warmed slowly to room temperature and stirred for 18 h. The resultant dark green solution was filtered from the insoluble graphite and potassium iodide. Concentration (to *ca.* 3 mL) and storage at room temperature for 18 h yielded **9** as dark green crystals. The mother liquor was decanted and the crystalline product dried under vacuum (230 mg, 67%). **Route 2:** Fresh strontium metal filings (0.29 g, 3.30 mmol) were suspended in 10 mL diethyl ether, and activated by the addition of a single crystal of iodine (*ca.* 5 mg), with stirring until the colour of the iodine had disappeared. A solution of $^{\text{Ph}}\text{Dimpy}$ (1.00 g, 1.65 mmol) in 10 mL toluene was then added to the mixture. The reaction mixture was stirred for 18 h at room temperature, and the resultant green solution was filtered from the excess metal. Volatiles were removed under vacuum, and the residue washed with 5 mL of hexane and dried under vacuum, yielding analytically pure **9** as a brown powder (712 mg, 62%). MP: >260 °C (dec.); ^1H NMR (300 MHz, C_6D_6 , 298 K) tentative assignments $\delta = 0.77$ (d, $J = 6.7$ Hz, 3H, $\text{CH}(\text{CH}_3)_2$), 0.87-1.34 (m, 45H, $\text{CH}(\text{CH}_3)_2$), 2.75 (m, 2H, $\text{CH}(\text{CH}_3)_2$), 2.85 (m, 2H, $\text{CH}(\text{CH}_3)_2$), 3.88 (m, 2H, $\text{CH}(\text{CH}_3)_2$), 4.84 (s, 1H, py-H), 4.90 (m, 2H, $\text{CH}(\text{CH}_3)_2$), 5.10 (m, 1H, py-H), 5.23 (m, 1H, py-H),**

5.34 (m, 1H, py-*H*), 5.49 (m, 1H, py-*H*), 5.50 (m, 1H, py-*H*), 6.42-7.37 (m, Ar-*H*); N.B. The very low solubility of the compound in non-coordinating solvents precluded the acquisition of meaningful ^{13}C NMR spectroscopic data; MS/EI m/z (%): 605.5 ($^{\text{Ph}}\text{Dimpy}^+$, 25), 432.3 ($^{\text{Ph}}\text{Dimpy-NDip}+2\text{H}^+$, 28) 264.1 (PhCNDip, 100), 176.2 (DipNH, 59); anal. calc for $\text{C}_{86}\text{H}_{94}\text{N}_6\text{Sr}_2$: C 74.47%, H 6.83%, N 6.06%, found C 74.35%, H 6.97%, N 6.12%.

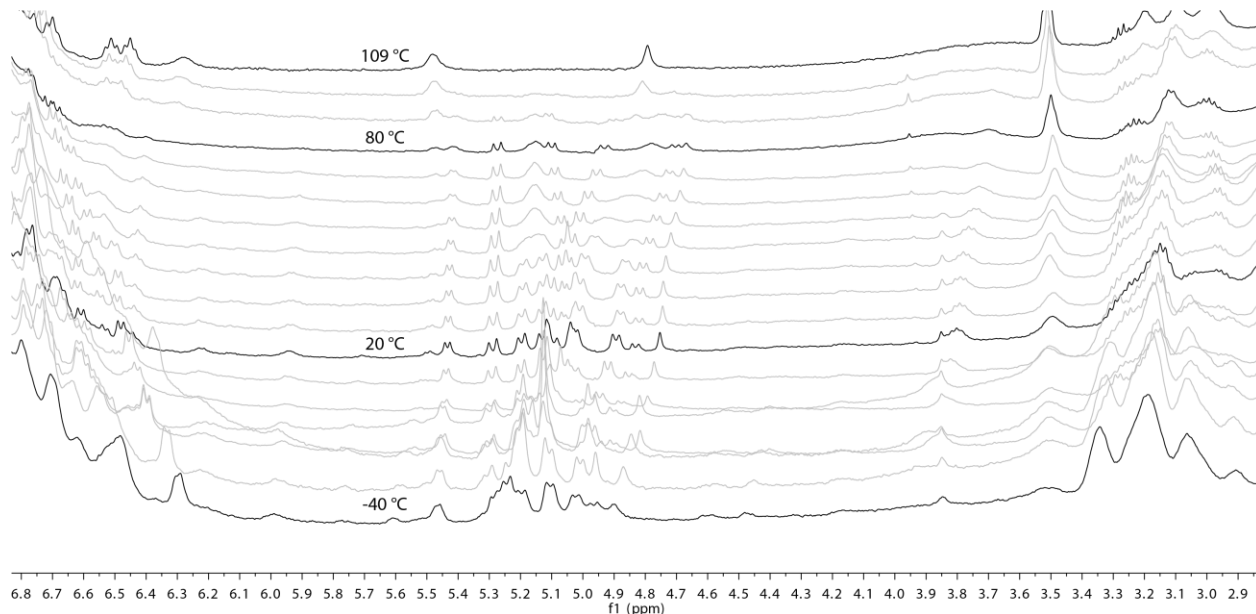


Figure S6. Variable temperature ^1H NMR spectra (300 MHz, toluene- d_8 , 298 K) of **9** collected between $-40\text{ }^\circ\text{C}$ and $109\text{ }^\circ\text{C}$.

Synthesis of [$\{^{\text{Ph}}\text{Dimpy}\}\text{Ba}\}_2$] **10.** Fresh barium metal filings (136 mg, 0.99 mmol) were suspended in 10 mL THF, and activated by the addition of a single crystal of iodine (*ca.* 5 mg), with stirring until the colour of the iodine had disappeared. A solution of $^{\text{Ph}}\text{Dimpy}$ (500 mg, 0.825 mmol) in 10 mL of toluene was then added to the barium suspension. The reaction mixture was stirred for 18 h at room temperature, and the resultant red solution was filtered from the excess metal. Concentration (to *ca.* 3 mL) and storage at room temperature for 18 h yielded **10** as dark red crystals. The mother liquor was decanted and the crystalline product dried under vacuum (360 mg, 59%). MP: $>260\text{ }^\circ\text{C}$ (dec.); ^1H NMR (400 MHz, toluene- d_8) tentative assignments $\delta = 0.70\text{-}0.77$, $0.88\text{-}1.04$, $1.11\text{-}1.14$, $1.18\text{-}1.22$, $1.34\text{-}1.44$ (m, 48 H, $\text{CH}(\text{CH}_3)_2$), 2.81 (sept., $J = 6.4\text{ Hz}$, 1H, $\text{CH}(\text{CH}_3)_2$), 3.04-3.25 (m, 4H, $\text{CH}(\text{CH}_3)_2$), 3.41 (m, 1H, $\text{CH}(\text{CH}_3)_2$), 4.67 (m, 1H, $\text{CH}(\text{CH}_3)_2$), 4.87, 4.99, 5.12, 5.19, 5.40, 5.88, 6.18 (7 x m, 7H, $\text{CH}(\text{CH}_3)_2$ and py-*H*) 6.57-7.38 (m, Ar-*H*), 7.70, 7.91, 8.25 (3 x m, 3H, Ar-*H*); N.B. The very low solubility of the compound in non-coordinating solvents precluded the acquisition of meaningful ^{13}C NMR spectroscopic data; IR (ν/cm^{-1} , ATR): 1570 (s), 1155 (s), 1175 (w), 963 (s), 920 (w), 878 (w), 829 (w), 806 (w); MS/EI m/z (%): 607.6 ($^{\text{Ph}}\text{DimpyH}_2^+$, 40), 432.3 ($^{\text{Ph}}\text{Dimpy-NDip}+2\text{H}^+$, 23) 264.1 (PhCNDip $^+$, 47), 176.2 (DipNH $^+$, 100).

N.B. A reproducible microanalysis of the compound could not be obtained due to its extreme air sensitivity, and difficulty in removing trace impurities after recrystallisation.

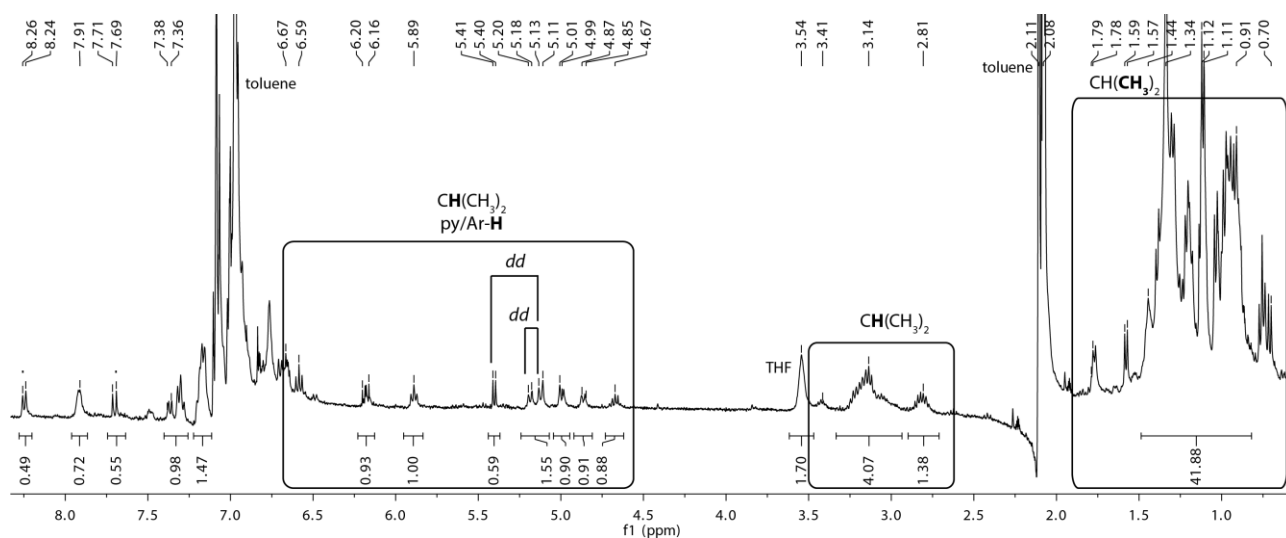


Figure S7. ^1H NMR (300 MHz, C_6D_6 , 298 K) spectrum of **10** showing tentative peak assignments.

2. X-Ray Crystallography

Crystals suitable for X-ray structural determination were mounted in silicone oil. Crystallographic measurements were made with a Bruker Apex X8 diffractometer using a graphite monochromator with Mo $\text{K}\alpha$ radiation ($\lambda = 0.71073 \text{ \AA}$), or the MX1 beamline of the Australian Synchrotron ($\lambda = 0.71090 \text{ \AA}$). The software package Blu-Ice⁴ was used for synchrotron data acquisition, while the program XDS⁵ was employed for synchrotron data reduction. All structures were solved by direct methods and refined on F^2 by full matrix least squares (SHELX-16⁶) using all unique data. Hydrogen atoms are typically included in calculated positions (riding model). Crystal data, details of data collections and refinements for all structures can be found in their CIF files and are summarized in Table S1.

Table S1. Crystal data for **4-10** and [(^{Ph}Dimpy)CaI₂].

	4	5	6	7
empirical formula	C ₄₃ H ₄₇ I ₂ MgN ₃	C ₄₃ H ₄₇ IMgN ₃	C ₄₇ H ₅₇ MgN ₃ O	C ₅₁ H ₆₃ MgN ₃ O ₂
formula weight	883.94	757.04	704.26	774.35
crystal system	monoclinic	triclinic	monoclinic	monoclinic
space group	<i>P</i> 2 ₁ / <i>c</i>	<i>P</i> -1	<i>P</i> 2 ₁ / <i>c</i>	<i>P</i> 2 ₁ / <i>c</i>
a (Å)	21.6350(9)	11.024(2)	8.3980(17)	9.6620(19)
b (Å)	21.6488(8)	14.654(3)	27.960(6)	25.268(5)
c (Å)	17.4647(6)	26.069(5)	17.207(3)	17.731(4)
α (°)	90	97.74(3)	90	90
β (°)	93.448(1)	100.95(3)	101.17(3)	92.75(3)
γ (°)	90	109.95(3)	90	90
V (Å ³)	8165.2(5)	3794.7(15)	3963.8(14)	4323.8(15)
Z	8	4	4	4
T (K)	1232	100(2)	100(2)	100(2)
ρ _{calcd} (g·cm ³)	1.438	1.325	1.180	1.190
μ (mm ⁻¹)	1.588	0.894	0.084	0.085
F(000)	3552	1564	1520	1672
reflns collected	92611	54901	54934	60960
unique reflns	15193	14091	7342	8035
R _{int}	0.1177	0.0775	0.0722	0.1384
R1 [I > 2σ(I)]	0.0386	0.0446	0.0461	0.0642
wR2 (all data)	0.0661	0.103	0.1169	0.1644
largest peak and hole (e·Å ⁻³)	0.79, -1.19	1.08, -0.91	0.18, -0.27	0.42, -0.33
CCDC no.	1994982	1994983	1994984	1994985

S 11

	8 •(toluene) ₂	9 •(toluene) ₂	10 •(toluene) ₂	[(^{Ph} Dimpy)CaI ₂]
empirical formula	C ₁₀₀ H ₁₁₀ Ca ₂ N ₆	C ₁₀₀ H ₁₁₀ Sr ₂ N ₆	C ₁₀₀ H ₁₁₀ Ba ₂ N ₆	C ₄₃ H ₄₇ CaI ₂ N ₃
formula weight	1476.09	1571.17	1670.61	899.71
crystal system	triclinic	triclinic	triclinic	monoclinic
space group	<i>P</i> -1	<i>P</i> -1	<i>P</i> -1	<i>P</i> 2 ₁ / <i>c</i>
a (Å)	10.553(2)	10.582(2)	10.538(2)	14.0702(10)
b (Å)	14.046(3)	14.100(3)	14.140(3)	19.2310(13)
c (Å)	14.758(3)	14.769(3)	14.454(3)	15.6894(12)
α (°)	92.22(3)	90	90	90
β (°)	108.48(3)	108.93(3)	75.31(3)	105.232(3)
γ (°)	97.02(3)	90	90	90
V (Å ³)	2052.2(8)	2067.4(8)	2077.5(8)	4096.2(5)
Z	1	1	1	4
T (K)	100(2)	100(2)	100(2)	123(2)
ρ _{calcd} (g·cm ⁻³)	1.194	1.262	1.335	1.459
μ (mm ⁻¹)	0.191	1.342	0.993	1.693
F(000)	792	828	864	1808
reflns collected	29592	35908	36107	53326
unique reflns	7592	9377	9458	7592
R _{int}	0.0556	0.0413	0.0513	0.1591
R1 [I > 2σ(I)]	0.0398	0.0359	0.0302	0.0589
wR2 (all data)	0.1068	0.0894	0.0759	0.1601
largest peak and hole (e·Å ⁻³)	0.29, -0.44	0.48, -1.05	0.66, -1.40	2.29 (near I2), -0.83
CCDC no.	1994978	1994979	1994981	1994980

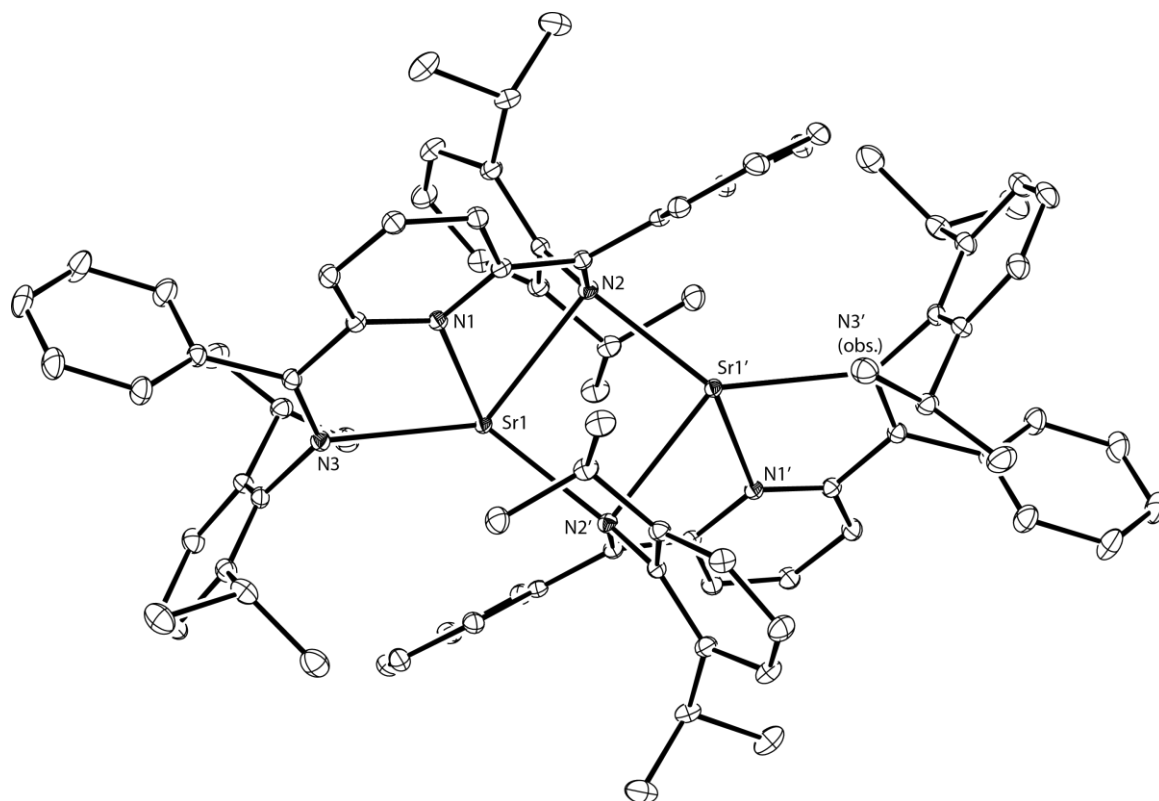


Figure S8. ORTEP diagram of compound **9** (25% thermal ellipsoids; hydrogen atoms omitted). See main text for metrical parameters.

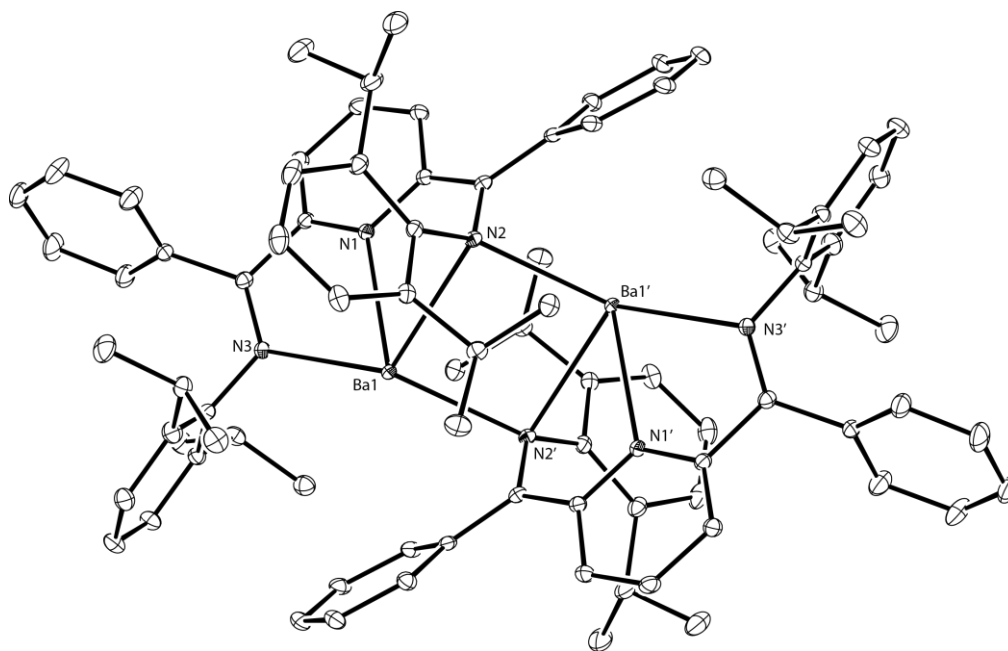


Figure S9. ORTEP diagram of compound **10** (25% thermal ellipsoids; hydrogen atoms omitted). See main text for metrical parameters.

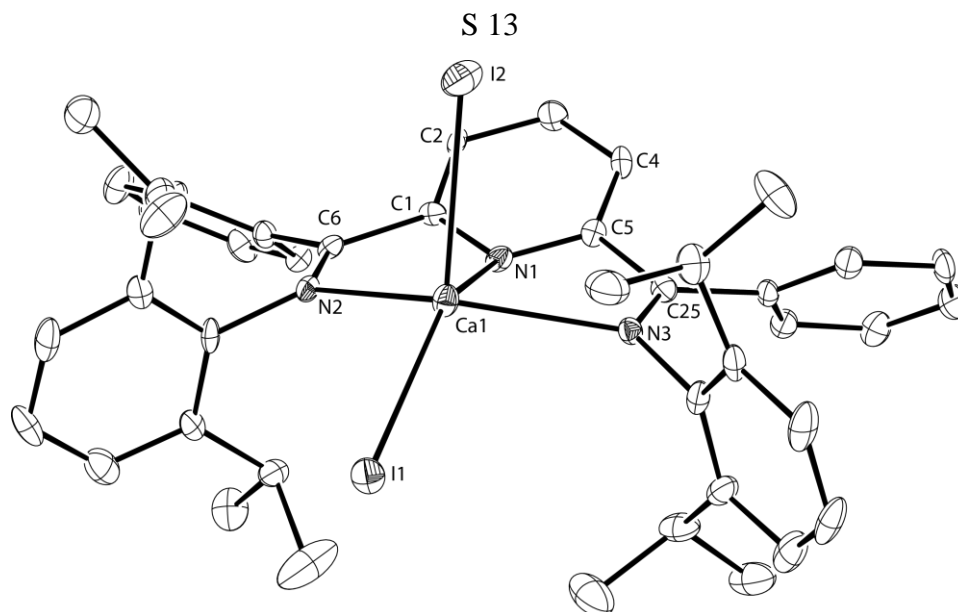


Figure S10. ORTEP diagram of compound $[(^{\text{Ph}}\text{Dimpy})\text{CaI}_2]$ (25% thermal ellipsoids; hydrogen atoms omitted). Selected bond lengths (\AA) and angles ($^\circ$): I(1)-Ca(1) 2.9605(18), Ca(1)-N(1) 2.411(6), Ca(1)-N(2) 2.520(6), Ca(1)-N(3) 2.531(6), Ca(1)-I(2) 3.0089(19), N(1)-Ca(1)-N(2) 65.8(2), N(1)-Ca(1)-N(3) 65.6(2), N(2)-Ca(1)-N(3) 128.0(2), I(1)-Ca(1)-I(2) 128.93(6).

3. Electrochemical Studies

Electrolyte preparation: Tetra(*n*-butyl)ammonium hexafluorophosphate ($[\text{Bu}^n_4\text{N}][\text{PF}_6]$; 98%, Beijing Health Science and Technology Co.) was recrystallised twice from ethanol before being dissolved in dry THF under a nitrogen atmosphere. The THF was removed briskly under vacuum at 60 °C to dryness. This process was repeated thrice to remove any remaining traces of ethanol and water. THF for electrochemical solutions was freshly distilled over molten potassium under a nitrogen atmosphere, before being freeze-pump-thawed degassed thrice to remove any trace amounts of oxygen. All solutions were prepared in J. Youngs ampoules in a glove box under a nitrogen atmosphere using recrystallised samples of the studied compound.

Electrochemical instrumentation and procedures: Electrochemical measurements were undertaken using either a BAS Epsilon electrochemical workstation or a custom-made Fourier Transformed ac voltammetry (FTacv) instrument (Monash University and La Trobe University, Australia)⁷ in three-electrode cells at ambient temperature (measured as 296 ± 1 K). All experiments were performed in a glove box under a high purity N_2 atmosphere. In voltammetric studies, the working electrode was a glassy carbon (GC; geometric surface area, $A = 0.067 \text{ cm}^2$) macrodisk electrode embedded in an isolating inert sheath (BAS) or a carbon fibre microelectrode (diameter, $d \approx 14 \text{ }\mu\text{m}$); auxiliary platinum wire electrode was confined behind the low-porosity glass frit. Oxidative bulk electrolysis experiments were performed in a three compartment cell with fine porosity glass frits separating the reference and auxiliary electrode chambers from the working electrode compartment; high surface area platinum gauzes were used as working and auxiliary electrodes. In all experiments, an AgCl-covered silver wire immersed in the same solution as in the working and auxiliary compartments was employed as a quasi-reference electrode. To calibrate the potential of the quasi-reference electrode, a small concentration of ferrocene (Fc^0) internal redox reference standard was introduced into the test solution, voltammograms were recorded, and the potential of the $\text{Fe}^{0/+}$ process was determined through experiment-simulation comparisons. Current data obtained with a GC electrode are normalised to the electrode surface area.

Electrochemical data were collected for 10 mM solutions of $[(^{\text{Ph}}\text{Dimpy})\text{Mg}(\text{OEt}_2)]$ (**6**), $[(^{\text{Ph}}\text{Dimpy})\text{M}]_2$ (M= Ca (**8**) and Ba (**10**)) in dry THF (0.3 M $[t\text{-Bu}_4\text{N}][\text{PF}_6]$). Results for **6**, **8** and **10** are discussed in the main text.

Simulations were undertaken using Monash Electrochemistry Simulator MECSim⁸ and commercial software package DigiElch 7.F. MECSim uses a planar diffusion model and was employed to derive parameters of the reversible potentials (E^0) and heterogeneous electron transfer rate constants (k^0). The simulated data presented below are based on these parameters, but were calculated using DigiElch 7.F and a mass-transport model based on a 2D diffusion towards a disk electrode.

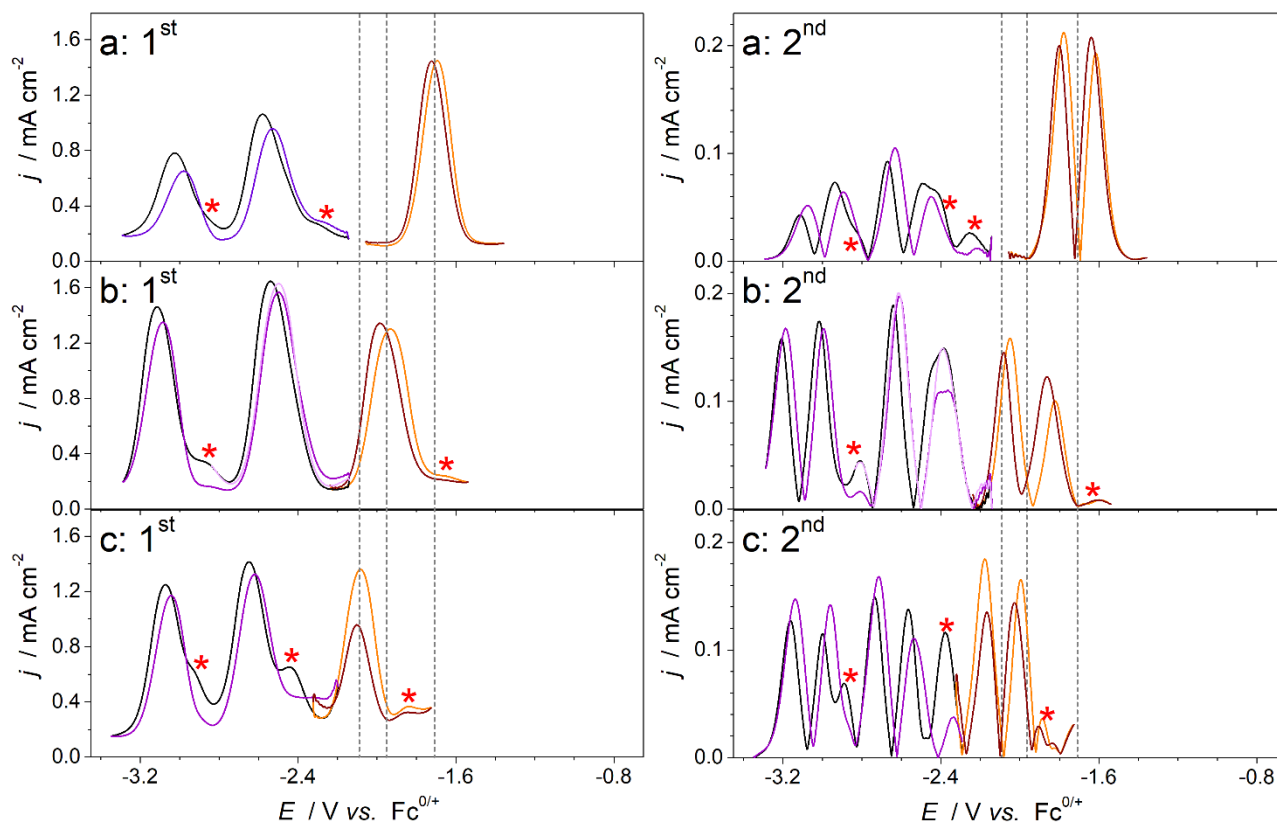


Figure S11. Fourier transformed ac voltammetric analysis of the reduction and oxidation of 10 mM (a) [$(\text{PhDimpy})\text{Mg}(\text{OEt}_2)$] (**6**), (b) [$(\text{PhDimpy})\text{Ca}$] $_2$ (**8**), and (c) [$(\text{PhDimpy})\text{Ba}$] $_2$ (**10**) in dry THF (0.3 M [Bu^n_4N][PF_6]) under high purity N_2 atmosphere using a glassy carbon electrode. Instrumental parameters: fundamental frequency, $f = 9.02$ Hz; amplitude, $\Delta E = 0.080$ V; scan rate, $\nu = 0.043$ V s^{-1} for two-electron reduction and $\nu = 0.045$ V s^{-1} for one-electron oxidation or reduction. Data are presented as envelopes for the first and second harmonic components derived from forward scans for one-electron oxidation (*orange*) and two-electron reduction (*black*), backward scans for one-electron oxidation (*brown*), two-electron reduction (*purple*) and one-electron reduction (*light purple*). Dashed lines are guides to an eye approximating the reversible potentials for one-electron oxidations. Asterisks denote signals not related to the major compounds.

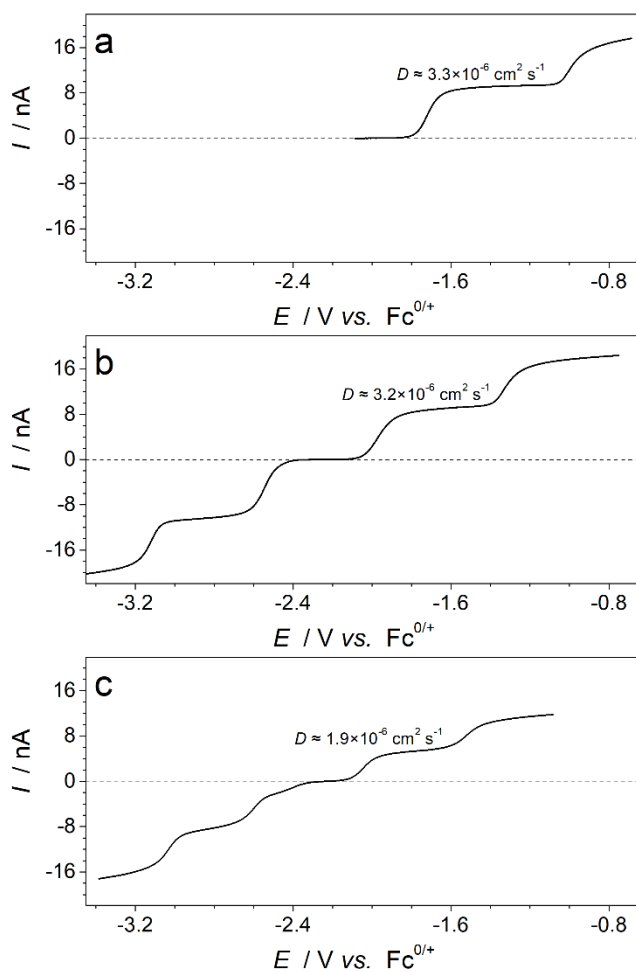
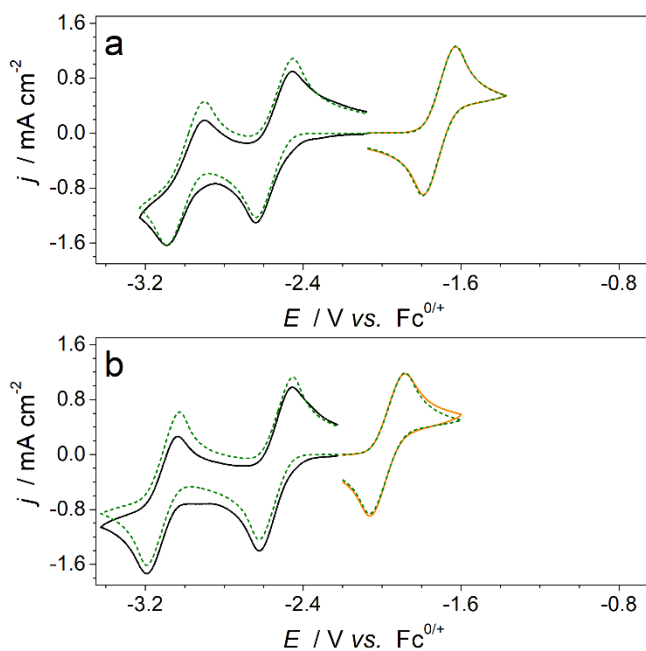


Figure S12. Quasi-steady-state voltammograms (scan rate, $\nu = 0.010 \text{ V s}^{-1}$) obtained for oxidation and reduction of 10 mM (a) [$(^{\text{Ph}}\text{Dimpy})\text{Mg}(\text{OEt}_2)$] (**6**), (b) [$\{(^{\text{Ph}}\text{Dimpy})\text{Ca}\}_2$] (**8**), and (c) [$\{(^{\text{Ph}}\text{Dimpy})\text{Ba}\}_2$] (**10**) in dry THF (0.3 M [$\text{Bu}^n_4\text{N}][\text{PF}_6$]) under high purity N_2 atmosphere using a carbon fibre microelectrode (radius *ca* 7 μm). Dashed lines are guides to an eye. Diffusion coefficients were derived from the diffusion limited currents for the first oxidation processes, though it is noted that the latter is not well defined, especially for **8** and **10**.



Compound	Process	E^0 / V vs. $\text{Fc}^{0/+}$	k^0 / cm s^{-1}	α
(6) $[(^{\text{Ph}}\text{Dimpy})\text{Mg}(\text{OEt}_2)]$	(6) ^{0/+}	-1.717	0.011	0.50
	(6) ^{-/0}	-2.541	0.005	0.50
	(6) ^{2-/1}	-2.975	0.003	0.50
(8) $\{(^{\text{Ph}}\text{Dimpy})\text{Ca}\}_2$	(8) ^{0/+}	-1.980	0.006	0.50
	(8) ^{-/0}	-2.535	≥ 0.05	0.50
	(8) ^{2-/1}	-3.092	≥ 0.05	0.50

Figure S13. Comparison of the experimental (*solid*) and simulated (*dashed*) dc voltammograms (scan rate, $\nu = 0.100 \text{ V s}^{-1}$) for the one-electron oxidation and two-electron reduction of 10 mM (a) $[(^{\text{Ph}}\text{Dimpy})\text{Mg}(\text{OEt}_2)]$ (6) and (b) $\{(^{\text{Ph}}\text{Dimpy})\text{Ca}\}_2$ (8) in dry THF (0.3 M $[\text{Bu}^n_4\text{N}][\text{PF}_6]$) under high purity N_2 atmosphere using a glassy carbon electrode. Table summarises key parameters for both compounds and each charge-transfer step. Other simulation parameters: $T =$ (a) 295 and (b) 297 K; double-layer capacitance, $C_{\text{dl}} = 1 \text{ } \mu\text{F}$; uncompensated resistance, $R_{\text{u}} =$ (a) 510 and (b) 550 Ω (estimated from the high-frequency electrochemical impedance data and by simulation of dc voltammograms for the oxidation of ferrocene assuming infinitely fast charge-transfer kinetics); 2D diffusion model for a disk electrode with an area of 0.067 cm^2 was used; diffusion coefficient for all species, $D =$ (a) 2.8×10^{-6} and (b) $2.6 \times 10^{-6} \text{ cm}^2 \text{ s}^{-1}$. All simulations are based on the simplest mechanisms involving one-electron charge transfer steps only; parameters for the first reduction step were derived from the analysis of voltammograms covering this process only (not shown) and then used for the analysis of the second reduction step.

4. References

1. T. Jurca, K. Dawson, I. Mallov, T. Burchell, G. P. A. Yap and D. S. Richeson, *Dalton Trans.*, 2010, **39**, 1266.
2. S. J. Bonyhady, C. Jones, S. Nembenna, A. Stasch, A. J. Edwards and G. J. McIntyre, *Chem. Eur. J.*, 2010, **16**, 938.
3. H. Podall, W. E. Foster and A. P. Giraitis, *J. Org. Chem.*, 1958, **23**, 82.
4. T. M. McPhillips, S. E. McPhillips, H.-J. Chiu, A. E. Cohen, A. M. Deacon, P. J. Ellis, E. Garman, A. Gonzalez, N. K. Sauter, R. P. Phizackerley, S. M. Soltis, P. Kuhn, *J. Synchrotron Rad.*, 2002, **9**, 401.
5. W. J. Kabsch, *Appl. Crystallogr.*, 1993, **26**, 795.
6. G.M. Sheldrick, *SHELX-16*, University of Göttingen, 2016.
7. A. M. Bond, D. Elton, S.-X. Guo, G. F. Kennedy, E. Mashkina, A. N. Simonov and J. Zhang, *Electrochem. Comm.*, 2015, **57**, 78.
8. G. Kennedy, A. M. Bond and A. N. Simonov, *Curr. Opin. Electrochem.*, 2017, **1**, 140.